ISSN 0252-1075
Research Report No. RR-045

CONTRIBUTIONS FROM

INDIAN INSTITUTE OF TROPICAL METEOROLOGY

HIGH RESOLUTION UV-VISIBLE SPECTROMETER FOR ATMOSPHERIC STUDIES

BY

S.BOSE, H.K.TRIMBAKE, A.L.LONDHE
AND
D.B.JADHAV.

PUNE - 411 005
INDIA

JANUARY 1991

RR-45

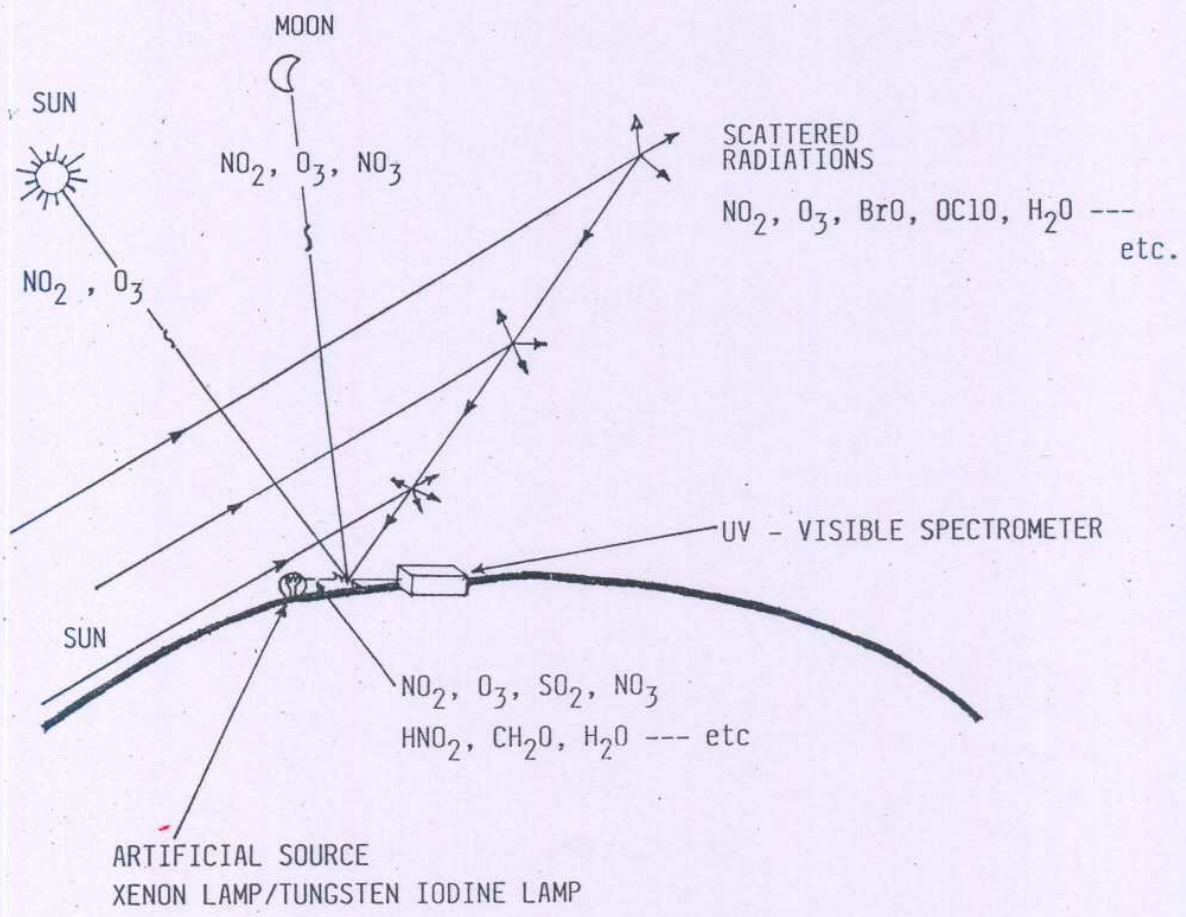
MOON
SUN
NO_2, O_3, NO_3
NO_2 , O_3
SCATTERED
RADIATIONS
NO_2, O_3, BrO, OClO, H_2O ---
etc.
UV - VISIBLE SPECTROMETER
SUN
NO_2, O_3, SO_2, NO_3
HNO_2, CH_2O, H_2O --- etc
ARTIFICIAL SOURCE
XENON LAMP/TUNGSTEN IODINE LAMP

PREFACE

For studies relating to the effect of greenhouse gases such as CO_2, NO_x, O_3, CFC's, CH_4 etc. on Earth's climate, extensive measurements of these trace gases in the atmosphere are essential. Advanced remote sensing techniques play a major role as far as the collection of basic information is concerned. Spectroscopy is one of such techniques that is being used for measurement of trace gases.

A high resolution UV-visible spectrometer has been developed at the Indian Institute of Tropical Meteorology, Pune. The principle of the spectrometer closely resembles to that of Czerny Turner-Ebert Fastie Spectrometer. It is designed, fabricated and tested at the Institute. Although this spectrometeric system is presently being used for monitoring stratospheric NO_2 and O_3, with appropriate modification, it has a capability to monitor other species like NO_3, OClO, BrO, H_2O .. etc in the stratosphere and NO_2, NO_3, O_3, CH_2O, SO_2, HNO_2 .. etc in the troposphere. This report contains the technical details of the optics and related electronics used in the spectrometer.

CONTENT

1. INTRODUCTION

The visible and infrared absorption spectrometry of the atmosphere using the Sun, the Moon and the Sky or artificial light (such as Xenon lamp, Tungsten lamp, laser beam) as a source has proven to be a powerful method of studying the total column density and the vertical distribution of atmospheric constituents for the last twenty years (Husson et al.,1985). For the understanding of the chemical and dynamical processes in the atmosphere, measurements of the different constituents in the atmosphere play an important role.

The atmospheric long geometric path obtainable at large zenith angles is a major factor, in increasing the sensitivity of spectroscopic measurements of trace constituents (Husson et al.,1985). Some of the species are not observable from ground and require high altitude platforms such as balloons, aircrafts or satellites. This also helps to minimize the interference by other species (especially H_2O). Although these measurements can be obtained by both insitu and remote sensing technique, the later is less expensive than the direct method.

For the possible usage of the technique of remote sensing, the high-tech spectrometers have been developed. Regular observations of the atmospheric constituents are being carried out by various scientists in different laboratories (Murcrary et al.,1983; Coffey et al.,1981; Solomon et al.,1987; Rowland et al.,1984; Syed and Harrison.,1981; McKenzie and Johnston.,1982; Carli et al.,1980; Platt and Perner, 1980; Girard and Louisnard, 1984).

Towards ground-based observations of atmospheric constituents in tropical countries there is an urgent need to develop high-tech spectrometers.

This report includes the detail information regarding design, fabrication and testing of the High Resolution Visible Spectrometer being developed at the Institute.

2. SELECTION OF OPTICAL SPECTROMETER FOR ATMOSPHERIC STUDIES

In spectroscopic studies of atmosphere, the scattering, emission or the absorption property of the scatterer is used to get the information of the medium i.e. to retrieve the atmospheric composition. The optical spectrometers for these studies are used either in static mode, (Solomon et al., 1987) or in scanning mode (Mckenzi and Johnston, 1982). Since during the atmospheric radiation studies the wide variations of the source intensities are observed, it is desirable to have high light gathering power (i.e. etendu) of the system (Jadhav, 1985).

From light gathering point of view 'Michelson-Fourier Transform' spectrometers are the most suitable in infrared spectral regions, 'IR GRILLE' spectrometer is also suitable for atmospheric monitoring (Girard and Louisnard, 1984). Grille spectrometer is less versatile than Fourier-Transform systems, but it is four to five time less expensive than the Fourier-Transform systems. However for atmospheric studies in visible spectral region the 'Grating Spectrometers' are more versatile and cost effective. Among the grating spectrometers as far as the light gathering and resolution are concerned (Fastie, 1953), the well known Czerny-Turner type of system with concave mirror and the Ebert-Fastie type of system with curved slit

have been found suitable. In this set up optical defects such as coma and astigmatism have been almost eliminated. The different atmospheric constituents those can be monitored by this system are outlined in Sec 6.

3. CZERNY TURNER-EBERT FASTIE SPECTROMETER

In any design of an optical system, it is essential to consider the detection threshold of the total set up along with the accuracies which can be achieved within the availability of the components in resources (Jadhav and Tillu, 1986). The design adopted is a combination of Czerny-Turner and Ebert-Fastie Spectrometer (Czerny-Turner, 1930; Fastie, 1953). The new combination has been designated as 'CZERNY TURNER-EBERT FASTIE' (CTEF) SPECTROMETER.

The system development is based on the selection of different components as per availability of the components within the resources. The ray diagram is shown in Figure 1. The light beam entering through the entrance slit S_1 is made parallel by the collimating mirror M_1 and is directed toward the plane diffraction grating G. The incident parallel beam is diffracted by the plane grating in different directions in the plane formed by the slits, mirrors and the grating. The parallel beam diffracted by the plane grating towards the telescopic mirror M_2 is focused on the focal plane of the telescopic mirror M_2 and passed through the exit slit S_2, is detected by the detector after focusing and passing through the order sorting filters (Figure 15).

3.1 SELECTION OF GRATING :

The selection criteria for this vital component depends upon the following two important factors.

(i) The resolving power which depends upon the product of the number of lines/mm (N) and the order of the diffraction (n), should be maximum for a required spectral region (Thorne, 1974). This however reduces the working range for the higher orders (more detail discussion is given in Sec 3.2)

(ii) The luminosity which is determined by the area of the grating and its blaze efficiency should be as large as possible for the region to be studied (James and Sternberg, 1969).

Table 1 explains the selection criteria of the grating, for the study of the visible spectral region. For the ruled type grating the priority is given to the grating with 1200 lines/mm blazed at 1.2 μ in first order. The holograpic gratings are found suitable for their better signal to back ground ratio and absence of the ghost orders (Bausch and Lomb Catalogue, 1983). Particularly the holographic grating with 2400 grooves/mm with high modulation in 2500-6000 A is found to be more suitable. However, while designing this spectrometer, due to non-availability of the holographic grating with above specifications, the ruled grating with 1200 lines/mm blazed at 1.2 μ for the first order was selected. This grating is specially ruled for working in higher orders.

For the selection of the size of the grating, the following points have been considered :

(i) Suitability of the selected size for atmospheric studies (e.g. for the

TABLE 1

List of Available Grating			Order of Diffr-action		n x (G/mm)		Overlapping in visible region		Remarks selection priority
Grooves/mm	Manfacturer	Blazed wavelength (Blazed Angle)	At 0.4 u	At 0.6 u	At 0.4 u	At 0.6 u	At 0.4 u	At 0.6 u	
600	B,D	5000 A 8°38'	1	1	600	600	No	No	No overlapping 5
	D	6320 A 10°56'	1	1	600	600	No	No	No overlapping 5
	D	1.2 u D 22° 1.25 u 24°17'	3	2	1800	1200	1.2 u I 0.6 u II	1.2 u I 0.4 u II	Avoidable overlapping 4
	B,D	1.6 u 28°41'	4	2	2400	1200	1.6 u I 0.8 u II 0.53 u III	1.8 u I 1.2 u II	Difficult to avoid overlapping
900	D	8000 A 23°0'	2	1	1800	900	0.8 u I	No	Avoidable overlapping 3
1200	D B	5000 A 17°27' 6000 A 22°	1	1	1800	900	No	No	Avoidable overlapping 2
	D B	1.2 u 46° 4' 1.25 u 48°35'	3	2	3600	2400	1.2 u I	1.2 u I	Avoidable overlapping 1

cond/.

List of Available Grating		Order of Diff-action		n x (G/mm)		Overlapping in visible region		Remarks selection priority
Grooves/mm Manufacturer	Blazed wavelength (Blazed Angle)	At 0.4 u	At 0.6 u	At 0.4 u	At 0.6 u	At 0.4 u	At 0.6 u	
1800 B,D	5000 A 26°45'	1	1	1800	1800	No	No	2* Larger size gratings not available (see catalogue)
2160 D	5000 A 32°4'	1	1	2160	2160	No	No	2* Larger size gratings are not available (see catalogue)
1800 B Holographic High Modulation	3500 A to 8000 A	1	1	1800	1800	No	No	No overlapping II*
2400 B Holographic High Modulation	2500-6000 A	1	1	2400	2400	No	No	No overlapping I**

* Larger size gratings are not available

** Selection priority for Holographic Gratings,

B - Baush & Lomb, (1986)

D - Diffraction Products (1983)

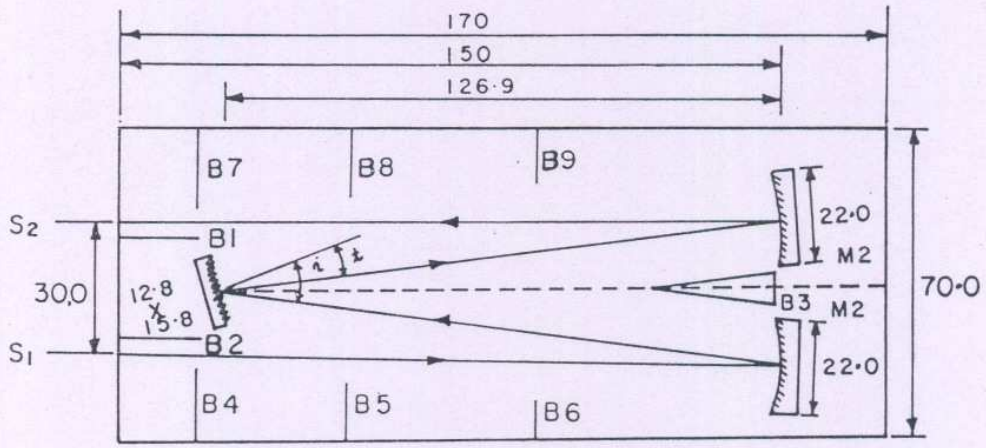

FIGURE 1 : RAY DIAGRAM OF CZERNY-TURNER EBERT-FASTIE SPECTROMETER

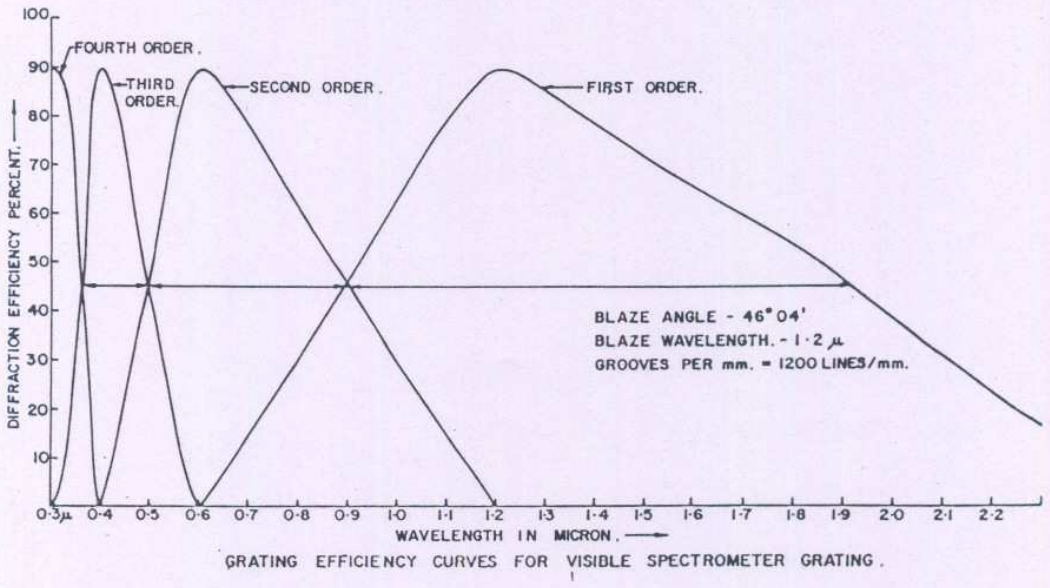

FIGURE 2 : DIFFRACTION EFFICIENCY CURVES FOR SPECTROMETER

study of wide range of sources like the Sun, the Moon, twilight sky or night airglow),

(ii) Availability of components like concave mirrors, slits, within the range of resources,

(iii) The size should not be too bulky as total system will also be large accordingly, and

(iv) Total cost of system should be reasonable.

The grating with following specifications has been selected for the present work.

Type : Plane diffraction grating,
Grooves/mm : 1200,
Size : 12.8x15.4x3 cm^3 (outer dimensions 13.5x16.5 cm^3), and
Blazed at : 1.2 μ 1st order, blazed angle 46 3'.

The grating efficiency curves drawn according to James and Sternberg (1969) are shown in Figure 2. One can decide this diagram for the suitable range of spectral region to be studied by a particular order (See Table 2 for the wavelength range which could be stuided with different orders). In actual practice, it is always useful to determine the blaze efficiency of the gratings experimentally, because in most of the cases the deviation in blaze efficiency is expected. However these calculations were carried out for the estimaion of our instrumental performance.

3.2 SELECTION OF ORDER SORTING FILTERS

For CTEF type of mounting, the grating equation can be given (Thorne, 1974) as

$$n\lambda = d\left[\sin(i) + \sin(r)\right] \text{- - - - - - - - - (1)}$$

where n : order of diffraction,
λ : wavelength of diffraction,
i : Angle of incidence,
r : Angle of diffraction, and
d : grating element i.e. the distance between two grooves.

From equation 1 it is clearly seen that for a set of angle of incidence i and the angle of diffraction r, for different orders the different wavelengths are possible, hence the overlapping of wavelengths is possible. To avoid this overlapping the order sorting filters are required (e.g at angle of incidence of 54 the wavelengths 1.2 μ, 0.6 μ, 0.4 μ & 0.3 μ are overlapping as in Figure 3).

Using the angle of incidence and the blaze efficiency, the diffraction efficiency curves are drawn in Figure 3 (Londhe et al.,1989) in which, wavelengths are also shown for the clarity. The short wave pass and the long wave pass square transmission type of filters have been selected for the system (Cat. Corion Corporation, 1983). For example, to study the spectral region 1.09 μ to 1.585 μ the long wave pass single filter at cut off wavelength 1 μ is suitable in the first order and in second order for the

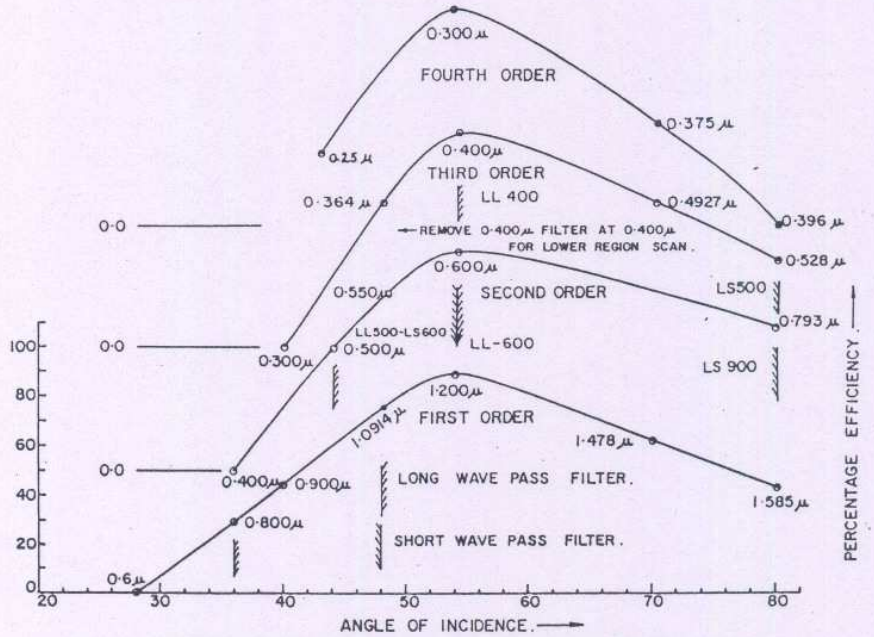

SELECTION OF ORDER SORTING FILTERS FOR VISIBLE REGION.

FIGURE 3

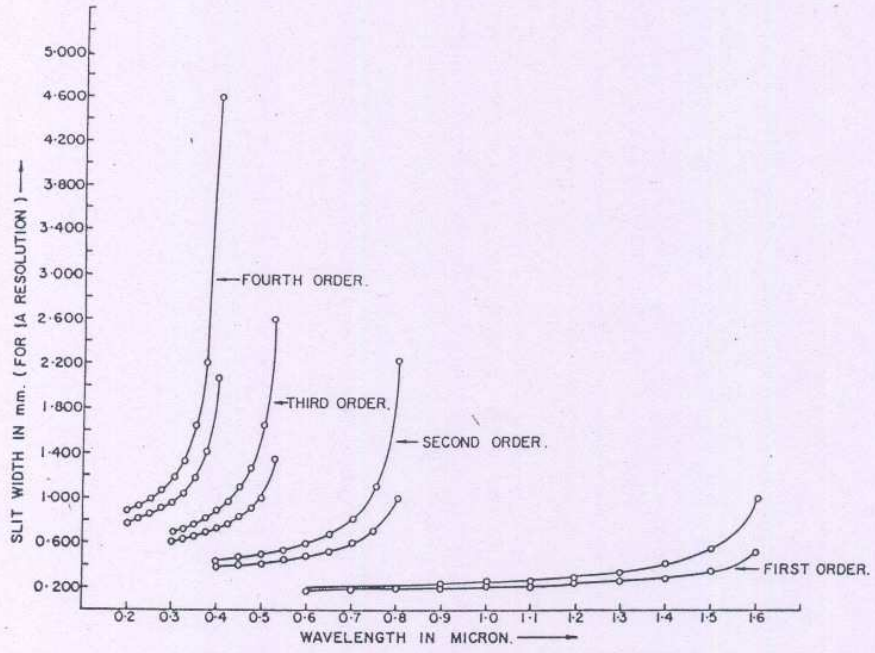

WAVELENGTH VS SLIT WIDTH FOR 1A RESOLUTION.

FIGURE 4

spectral region 0.6 μ to 0.9 μ the long wave pass filter at 0.6 μ cut off and short wave pass filter at 0.9 μ cut off are suitable. Thus one can select one or two optical filters for the suitable region and get the square wave transmission function for the region of interest.

3.3 CURVED SLITS :

Fastie (1952 a,b) has given an expression for the length (height) of the straight slit to give a minimum possible value for resolution (i.e. maximum resolving power).

$$L = 10 \lambda f^3 \quad - - - - - - - (2)$$

where L : Length of the straight slit to be determined,
λ : wavelength to be studied,
f : f number of the system, and
: focal length of mirror/apperature of the mirror (156/22 = 7.09, for the system).

From equation 2 the maximum height of the straight slit for the system at = 0.6 μ is 2.13 mm and the length of the curved slits (for the system) is nearly equal to the height of the grating i.e. 12.8 cm (Fastie, 1953).

Due to increase in the length of the curved slits, the light collecting efficiency of the system is increased by 60 times as compared to the straight slit configuration. The curved slits are also useful to eliminate the astigmatism and coma in the system (Fastie, 1952 a;b; 1953).

For the present system the estimated length of the curved slit is 12.8 cm. However, a slit of height 15 cm is actually prepared, and the central portion of 12.8 cm height was used to eliminate the errors arising due to the end portions of the slit. The diameters of the curved slits are determined by the minimum allowable distance between the centres of two concave mirrors used in the spectrometer (Jadhav and Tillu, 1986). In this case, from ray tracing, the diameter of the single mirror is 22 cm. The minimum possible distance between the centres of two mirrors is 30 cm which is the minimum distance required to mount 22 cm diameter mirrors. Hence the diameter of the curved slit is taken as 30 cms.

3.4 FOCAL LENGTH OF THE MIRRORS :

The Ebert-Fastie is a near littrow type of mounting and the slit width W can be given (Fastie, 1952) as,

$$W = \frac{F \, d\lambda \tan \alpha}{\lambda} \quad - - - - - - - (3)$$

where F : Focal length of the concave mirror,
α : the blaze angle,
λ : the blaze wavelength of the grating, and
d : spectral band pass.

Equation 3 can be used as first approximation for estimating the optimum

values of W and F. It is obvious that optimization depends upon two opposite requirements e.g. if value of $d\lambda$ is small by choosing large F for higher resolving power, the luminosity and the available signal will be small and vice versa.

The minimum slitwidth, which can be manufactured, is required for deciding the focal length of the mirrors for achieving higher resolving power of the system. The higher the focal length of the mirror higher is the dispersion of the system, but throughput of the system also reduces i.e the light gathering power is reduced. Taking into consideration these two opposite criteria (dispersion and the light gathering power), the focal length found suitable for the system is 150 cm.

3.5 MIRROR, GRATING AND THE SLIT POSITION :

The optical layout of the system is shown in Figure 1. The curved slits are placed at the focal plane of the respective concave mirrors (Fastie, 1953). The distance between the grating to the concave mirror is kept as 0.846 times the focal length of the concave mirrors according the Sassa's (1961) formula, for the minimum astigmatism and coma. This distance comes to 126.9 cm for the present set up. The separation between the centres of two concave mirrors and distance between the two mirrors is selected according to procedure laid down in Sec. 33.

To avoid the instrumental scattering, the use of baffles is essential with the following conditions :

(i) The entrance and the exit slit should not see the telescopic and the collimating mirrors respectively,

(ii) The entrance or the exit slit should not directly see the grating, and

(iii) The maximum projected area of the grating should only be open for the mirrors; other area should be covered by the suitable apertures .

The intermediate reflection in the system should also be avoided by the baffles. The number of baffles used at different places are shown in Figure 1. The projection of the beams at their extreme positions is taken into consideration to decide the shape of the baffles. The inner surface of the system other than the optical components are covered by anti reflecting black surface such as velvet cloth or dull black paint.

3.6 SLIT WIDTH RELATION :

Although the widths of entrance and the exit slits are kept constant during the observation schedule, it is necessary to know the inter relations between the slit widths. The slit width changes at constant resolution for different spectral regions and there is considerable difference at constant resolution in the widths of the entrance and exit slits. The expression for the entrance slit width (dsi) and the exit slit width (dsr) are given (James and Sternberg 1969) as

$$dsi = \frac{2\, d\lambda\, F}{\lambda(\cot\beta + \tan r)} \qquad \text{------ (4)}$$

$$dsr = \frac{2 d\lambda F}{\lambda(\cot\beta - \tan r)} \quad \text{- - - - - - - - (5)}$$

where λ is the wavelength to be studied

B = θ + r, where r is the angle of diffraction

θ : is the angle between the incidence ray and the optic axis (which is 6.74) for this case).

r = Ebert angle (which is 5.71 for this case)

The values of dsi and dsr were evaluated for different values of wavelengths and illustrated in Figure 4. To acheive high resolution and high light collection efficiency, it is necessary to adjust the slit widths according to above calculations. For atmospheric studies, the resolution of the order of an angstrom is sufficient. Hence for these calculations, $d\lambda$ can be fixed as 1 A however for higher or lower $d\lambda$ values the slit widths calculated will be directly proportional to the values under consideration (e.g. for working at 0.5 μ the third order is suitable, as the higher slit widths are possible at the same 1 A resolution (widths of the entrance and exit slit are 0.85 mm and 1.3 mm respectively). However, in actual practice for 0.85 mm slit width for both the slits, the resolution of 1 A is only possible, as the output is the effect of convolution of the entrance and exit slit functions. The reduction in width of exit slit (compared to calculations) reduces the throughput of the system by 1.5 times. These relations are useful when the signal-to-noise ratio is poor.

3.7 DISPERSION OF THE SPECTROMETER AT DIFFERENT ORDERS :

The dispersion of the spectrometer is calculated according to equation 5. The dispersion curves for different orders and different wavelengths are shown in Figure 5. For higher orders the dispersion of the system improves (i.e dispersion, A/mm reduces) as wavelength increases for any one order.

The minimum adjustable slit width for the system is 25 μ $\pm$ 5 μ. Thus calculations have been carried out for the maximum achievable resolution at 25 μ slit width. In Table 2 the range of maximum resolution that can be achieved by the system is shown. It is seen that resolution of the system reduces for lower orders.

3.8 THROUGHPUT OF THE SPECTROMETER

The photon flux that can be collected from an extended source is governed by an instrumental parameter known as light grasp or throughput T (Fastie 1967), which is equal to the product of the effective collecting area of the grating A', the transmission T, and the collecting solid angle, Ω of the system.

$$T = A' T \Omega = (A\cos i)(R^2 B)\left(\frac{WL}{F^2}\right)$$

$$= WL(R^2 B)(A\cos i/F^2) \quad \text{- - - - - (6)}$$

where R is the reflectivity of the mirror which is taken as 0.9 (for the

Table 2 : Maximum resolution can be achieved by high resolution visible spectrometer with 25 μ slit width

Order of Diffraction	Wavelength Range	Resolution Range
1	0.8 μ to 1.5 μ	0.1125 A to 0.0475 A
2	0.5 μ to 0.8 μ	0.0500 A to 0.018 A
3	0.4 μ to 0.5 μ	0.0250 A to 0.0125 A
4	0.3 μ to 0.4 μ	0.0200 A to 0.0063 A

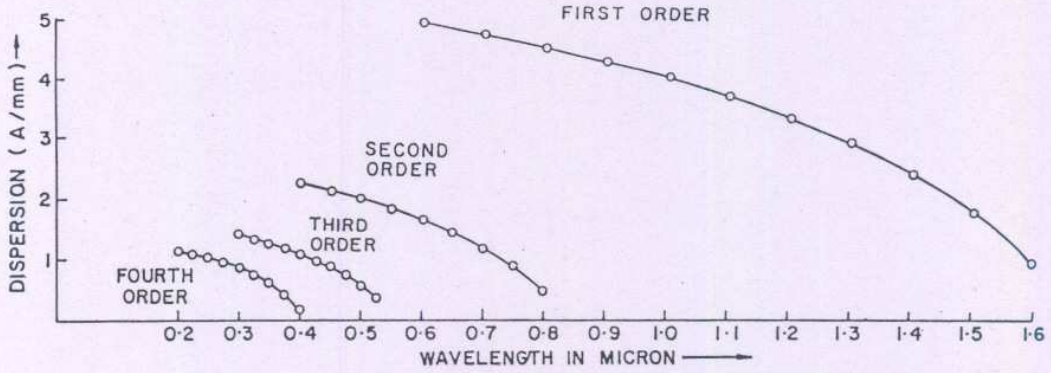

WAVELENGTH VS DISPERSION OF VISIBLE SPECTROMETER FOR DIFFERENT ORDERS.

FIGURE 5

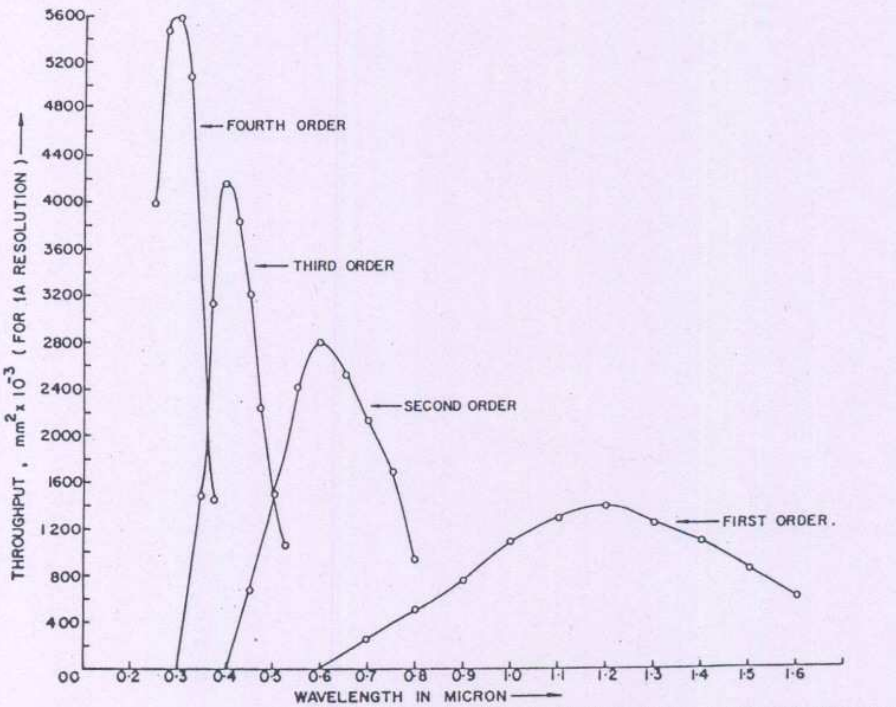

THROUGHPUT VS WAVELENGTH (FOR VISIBLE SPECTROMETER)

FIGURE 6

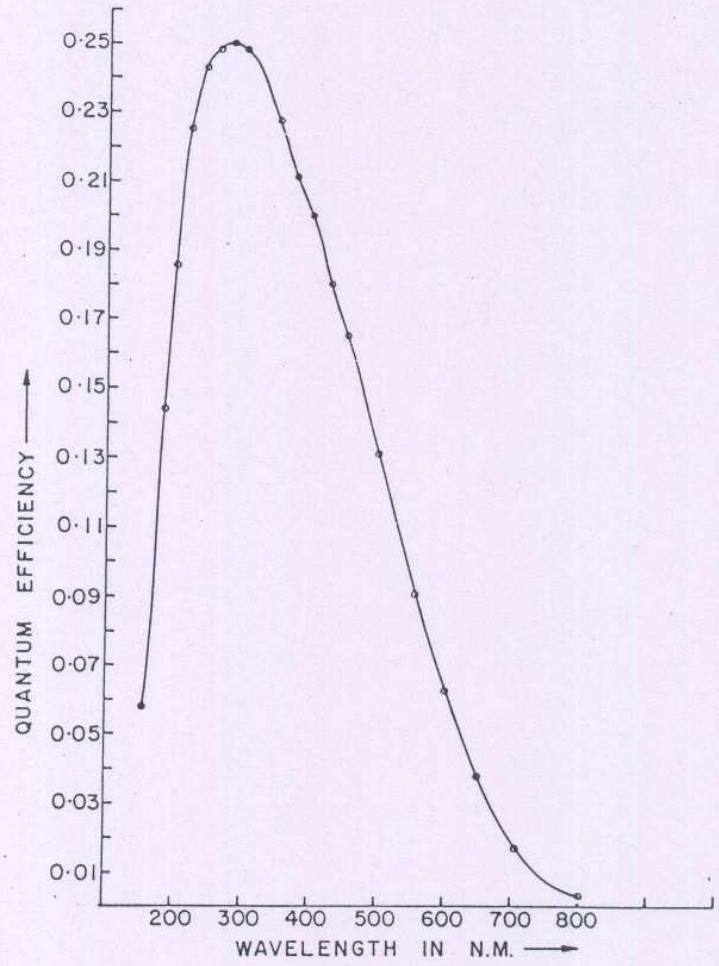

FIGURE-7: QUANTUM EFFICIENCY VS WAVELENGTH.
(FOR PHOTO MULTIPLIER TUBE
HAMAMATSU R 763.)

FIGURE 7

alluminium coated mirrors)

where B : is the diffraction efficiency of the grating which is estimated from the curve shown in Figure 2.,
W : Slit width,
A : Area of grating = 12.8x15.4 cm^2,
L : Slit height,
F : Focal length of the concave mirrors.

The throughput of the system as a function of wavelength for 1 A spectral band pass has been worked out using above equations and is shown in Figure 6. It is seen from the curve that the throughput is high for higher orders, and also the curves give more ideas regarding the use of the order of the grating for a particular spectral region. For example, from the diffraction efficiency curve of the grating it is found that, for the second order the useful spectral region is 0.5 μ to 0.8 μ but from throughput curves the useful spectral region for the second order is 0.49 μ to 0.83 μ. Thus the throughput calculations are useful for deciding the working range of different orders.

The signal in photoelectrons for any detector, in general, is given (Fastie, 1967) as

$$S = B_S T Q \text{ - - - - - - - (7)}$$

where B_S : the brightness of the source in photons $cm^{-2}sec^{-1}str^{-1}$
Q^S : Quantum efficiency of the detector.

Equation 7 is used to obtain the output of the photomultiplier tube in photoelectrons. For the current system the Hamamatsu photomultiplier tube R-763 sensitive in UV region with sensitivity better than S 20 spectral response (Hamamatsu Cat.) is used. The Quantum efficiency curve for the tube has been calculated (according to Hamamatsu Catalogue 1988) and is shown in Figure 7. It is seen in Figure 7 that the tube R 763 has good Quantum efficiency from 1800 A (UV Region) to 7000 A (Near IR) region.

The signal in photoelectrons with the corresponding wavelength is also calculated for a source intensity 1 KR/A and is shown in Figure 8. From these calculations it is clearly seen that for the system with photomultiplier tube as detector the photoelectron output shows increasing trend from 3rd to 4th order.

3.9 WAVELENGTH SCANNING SYSTEM :

The visible spectral region is generally scanned linearly in wavelength scale and the wavelength linearity can be achieved by the sinedrive type of system (James and Sternberg 1969).

From equation (1) (using trigonometric relation)

$$n\lambda = 2d \sin\left(\frac{i+r}{2}\right) \sin\left(\frac{i-r}{2}\right) \text{ - - - - - (8)}$$

The equation (8) is important for the Czerny Turner-Ebert Fastie system

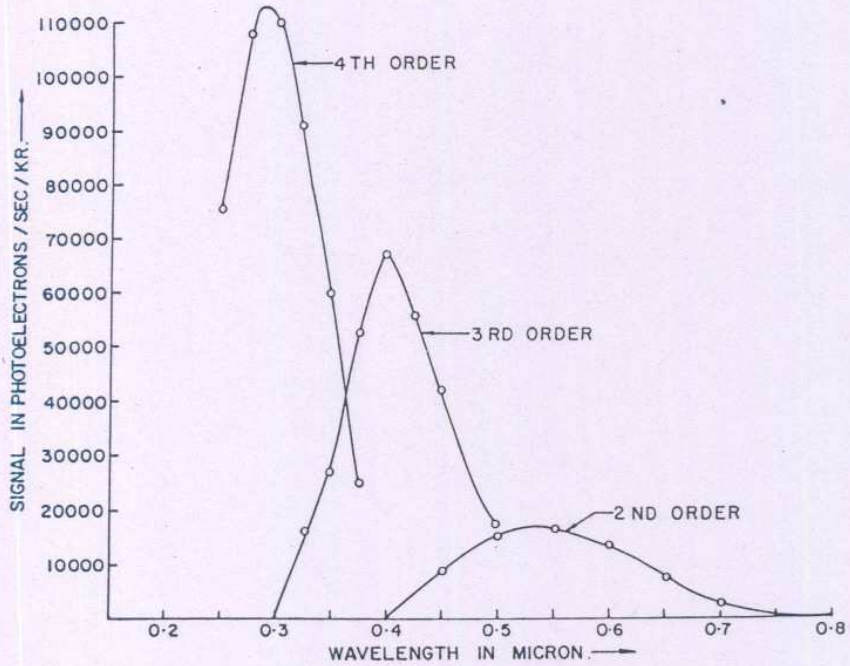

FIGURE 8

SIGNAL IN PHOTOELECTRONS VS WAVELENGTH
(PHOTOMULTPLIER TUBE HAMAMATSU R763)

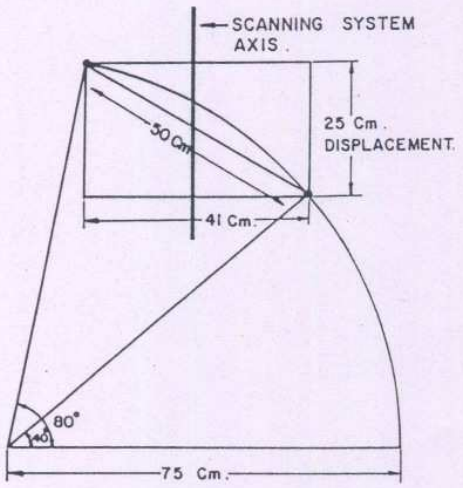

FIGURE 9

ACTUAL REQUIRED SCANNING OF VISIBLE SPECTROMETER FOR SINE DRIVE MECHANISM (DISPLACEMENT OF SCREW IS DIRECTLY PROPORTIONAL TO THE WAVE LENGTH.)

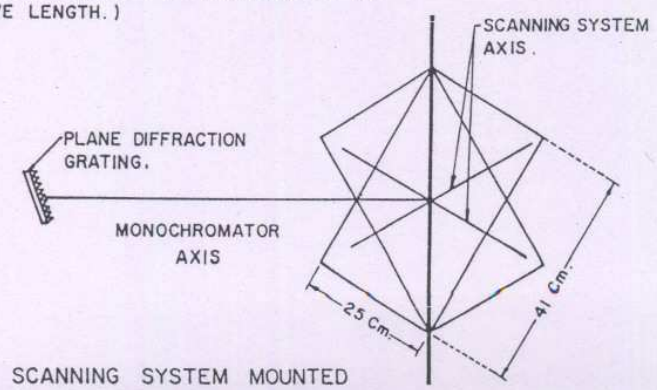

SCANNING SYSTEM MOUNTED ON MONOCHROMATOR AXIS.

as (i-r) is constant for the system.

$$\lambda \propto \sin\left(\frac{i+r}{2}\right) - - - - - - - - (9)$$

Thus the displacement of the lead screw can be made proportional to the wavelength.

To achieve the rotation of the grating proportional to the wavelength the grating is rotated by a lever attached at central axis of the grating in such a way that the displacement of the lever is proportional to the sine of the angle of rotation of the grating. This can be achieved by resting the translating lever on the smooth surface which is to be displaced by nut and screw arrangement.

The linear wavelength scale and wavenumber scale have been discussed by various authors (James and Sternberg, 1969; Badger, 1948; Thorne, 1974). For scanning the complete spectral region, as shown in Figure 4, the grating is to be rotated from 40° to 80° of the angle of incidence. For scanning the complete spectral region of the available high resolution system 50,000 sample points are required. To work for these sample points a stepper motor driven system with 250 mm displacement is to be rotated through 40° to 80° of grating by linear wavelength scale (Figure 9.a). However, the same displacement and the rotation of the grating can be achieved by rotating the axis of the scanning system (Figure 9.b). While deciding the orientation of the scanning system, the condition of the displacement of nut and the angle scanned are taken into account. Thus, by placing scanning system at any location and adjusting the orientation of the scanning system the linearity in wavelength scanning can be achieved.

4. MECHANICAL DESIGN AND CONTROL ELECTRONICS :

The detailed mechanical design and the control electronics of the system are discussed below.

4.1 CURVED SLITS :

The curved slits with stainless steel jaws have been fabricated with height and radius of curvature 15 cms each. (Figure 10 [a,b]). The slit jaws are held by the 'Square lever frame assembly'. Four strips of the lever are rivetted in such a way that the lever operation should be smooth. The opening/closing of the slit is performed by the movement of the lever frame assembly.

The movement of the lever frame is guided by the sliders, which are mounted in grooves in such a way that these sliders slide inside the grooves while opening the slit. The lever assembly and the slit jaws are mounted on a stepped circular disc with aluminium covers to avoid light interference from outside.

A micrometer screw is mounted on one of the sliders. The opening/closing of the slit is performed by rotating this screw. The slit width is calibrated using the travelling microscope. The minimum opening of the slit measured by the micrometer is 10 μ and the maximum opening of the slit can be kept as 10 mm. Hence the slit can be adjusted from 0.0 to 10 mm with 10 μ least count.

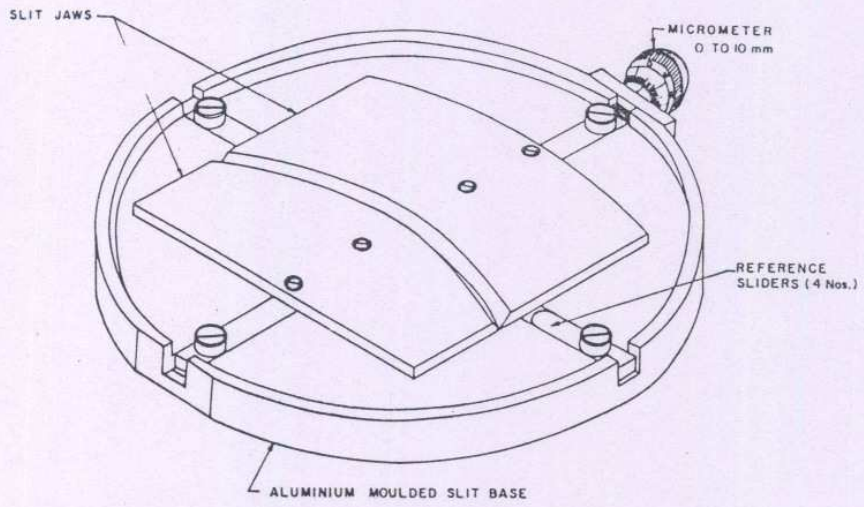

(a)

INSIDE - VIEW OF CURVED SLIT

	DRN	V.V. Deodhar
	TRD	V.V. Deodhar
DRG. NO. LIP-M-1001	CHD	
	Scale 1:1	
I. I. T. M. PUNE-8		

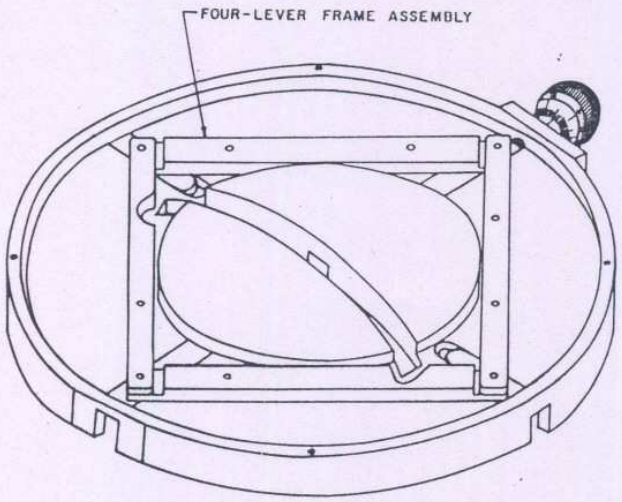

(b)

BACK-VIEW OF CURVED SLIT

	DRN	V.V. Deodhar
	TRD	V.V. Deodhar
DRG. NO. LIP-M-1002	CHD	
	Scale 1:1	
I. I. T. M. PUNE-8		

FIGURE 10

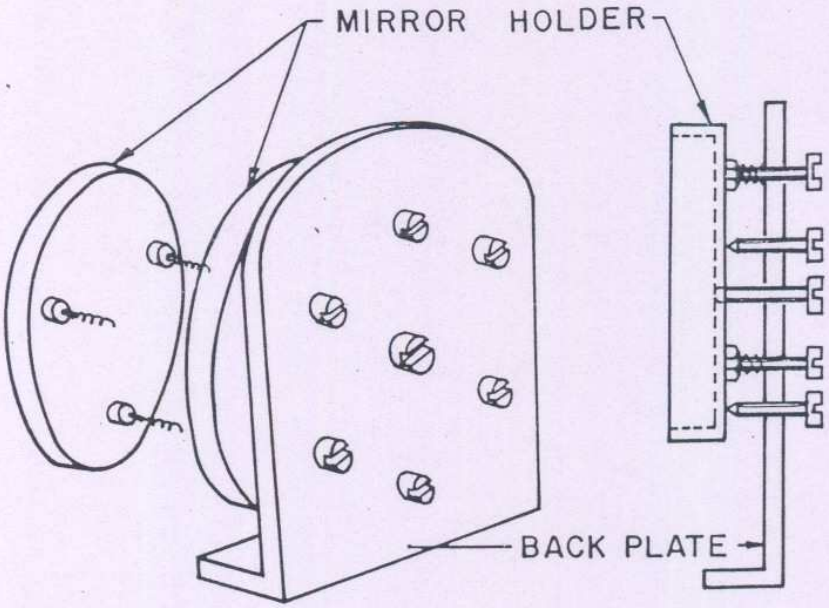

FIGURE 11

MIRROR MOUNT

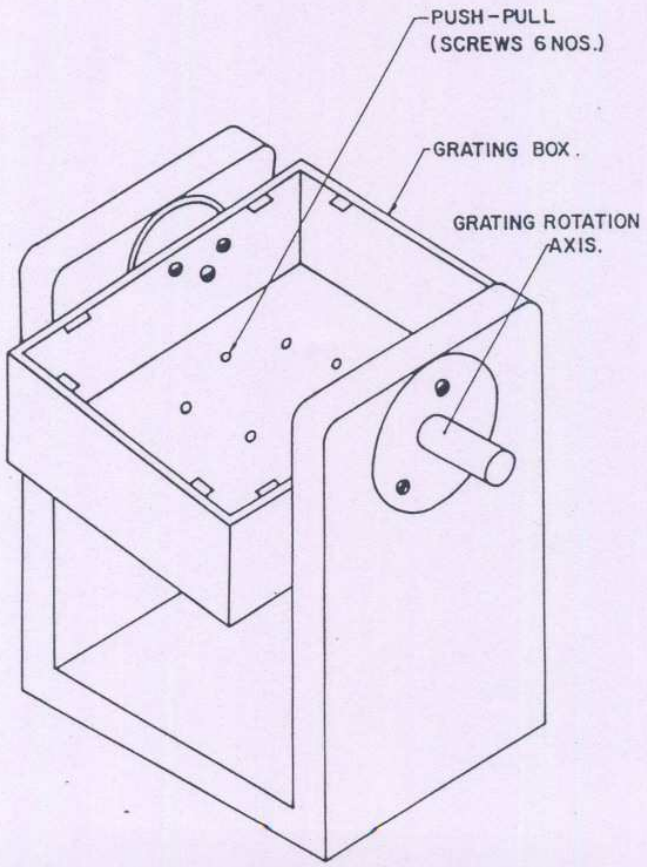

FIGURE 12

GRATING MOUNT.

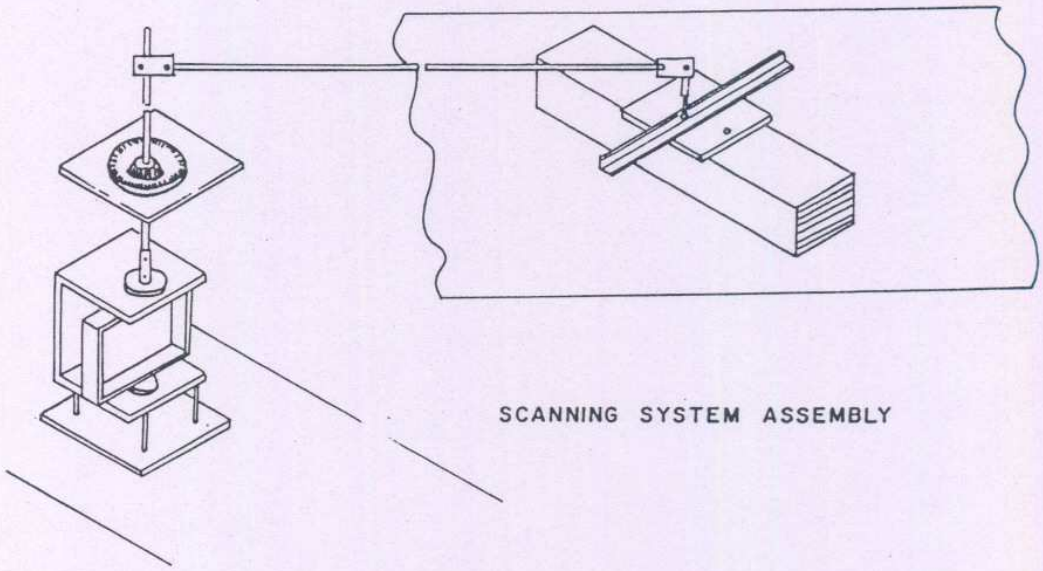

SCANNING SYSTEM ASSEMBLY

FIGURE 13.

DATA ACQUISITION / CONTROL FOR A SPECTROMETER (BLOCK DIAGRAM)

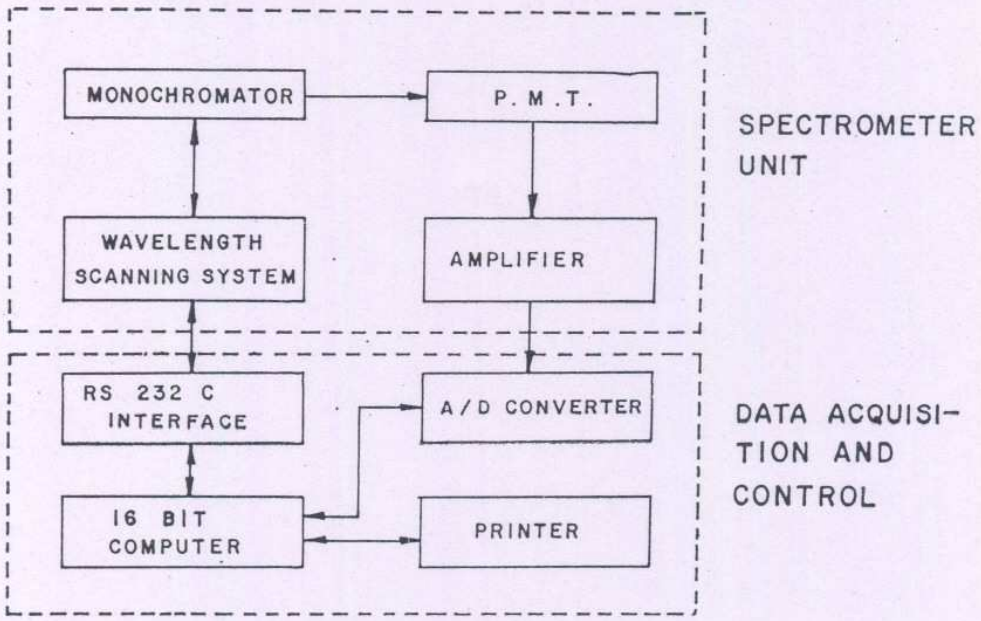

FIGURE 14

4.2 MIRROR MOUNT :

The mirror of 22 cm diameter and 3 cm thickness is mounted in a circular holder which is held at the back support plate by 3 sets of push pull type of screws. One permanently fitted screw is provided at the centre of the holder to avoid accidential release of the mirror holder by the spring loaded screws of push pull arrangement. Three screws with spring tension are used to align the plane of the mirror and remaining three are used to fix the aligned position of the mirror as shown in Figure 11.

4.3 GRATING MOUNT :

The grating box is held by two axes mounted on the bearing and the C type holder. The grating plane and parallelism of the grooves with incidence ray plane can be achieved by the set of screws mounted at the bottom and sides of the grating box.

The C-type holder and grating box are moulded in LM 6 aluminium. C-type holder is fitted to the monochromator box by the 4 M10 screws. The mount is sufficiently sturdy and remains in its position so that the alignment of the grating does not change during vibrations and jerks. The grating box is rotated by a rod attached to grating axis and scanning system. The design of the grating mount is shown in Figure 12.

4.4 SCANNING SYSTEM

The steel bar (whose centre passes through the plane of the grating) is mounted on the double bearing system on which a Bevel Protector is mounted with least count of 5 minutes. The grating rotation can be monitored visually. The scanning arm lever is attached to this steel bar which rests on the translating glass plate by the help of a spring tension. The schematic diagram is shown in Figure 13. The unislide assembly for the translation of the nut is procurred from Velmex, Corp, USA. The single step of five micron displacement can be achieved with the help of control electronics and stepper motor of the scanning system. The scanning system can be coupled with multichannel averager with RS 232 C port.

4.5 CONTROL ELECTRONICS :

A multichannel averager with control system is procurred (from M/s. Dynalab, India) as per the necessary requirements planned for the analysis of the spectroscopic data.

The block diagram of the system is shown in Figure 14 and the specifications of the system are as follows :

i. 640 KB RAM,
ii. 1x20 M Byte Hard Disc,
iii. 1x360 K Byte Floppy Disc,
iv. Monochrome Monitor,
v. Key Board,
vi. 100 microsecond 14 bit A/D Conventor,
vii. Control for, a. Two shutters, b. Six filters (2 sets).
viii. 160 CPS-132 Column Matrix Printer.

The following functions can be carried out by using the above system.

i. Control commands for the wavelength drive assembly so as to set wavelength limits for each scan, scan speed, number of scans, step intervals,

ii. Shutter control and provision for selection of either of the two shutter or both,

iii. Control for selection of filters by number, and

iv. Data processing for the conversion of data from the analog output to digital output (A/D) with

a. conversion rate depending on scan speed (interactive),

b. maximum conversion speed-1000/sec, with 14 bit conversion accuracy,

c. storage of converted data in computer memory,

d. option, for averaging A/D output over several scans during slow scans (Maximum 100 scans),

e. storage of data converted in Radom Access Memory prior to final storage on disk,

f. Provision for 50,000 data points during each scan,

g. Integration of data from subsequent scans,

h. Provision for integrating upto 100 such scans

i. Display of each scan graphically on CRT.

j. Display of the numeric value on the screen with provision of a matrix printer for printing output plots of scans, Numeric values of spectral measurements, and Result of any analysis.

v. Provision of the software for

a. Auto/Manual use of instruments,

b. Two control outputs are provided for closing the entrance and exist slits for dark current monitoring,

c. Provision for computing ratios of measured scanns and reference scans, and

d. Data is stored floppy disks in IBM compatible format.

vi. The maximum operating capacity of the system is such that the data will be recorded in 50 K locations for one scan, for the next scans the data will be added in corresponding memory locations of the wavelengths. This reduces total memory locations for number of scans compared to storing each scan separately. The provision is made for adding maximum 100 such scans for additions.

The above control and data acquisition system can acquire data from two spectrometers alternately. This provision is made for the operation of high

resolution visible spectrometer and infrared Grille - Spectrometer which are being developed at the Institute.

5. SETTING OF THE SPECTROMETER

5.1 ALIGNMENT OF MIRRORS, GRATING & SLIT

The concave mirrors are grinded and polished upto $\lambda/4$ surface accuracy at 5893 A and are tested by Ronchi test (considered to be standard test). The radius of curvature is also measured by Ronchi method. The radius of curvature of one mirror is 149 cm and that of other is 151 cm. The alignment of concave mirrors is carried out by autocollimation technique using a plane mirror. The plane of the mirror is adjusted with reference to the height of the incident image of the slit.

The grating is rotated through a small angle by adjusting screws provided to support the grating. This alignment is considered to be useful to adjust the lines of the grating in the vertical plane of the slit. The grating plane and mirror planes are adjusted in such away that all the orders coincide exactly on the exit slit.

The slit widths have been measured by travelling microscope during the opening and closing of the slit. The micrometer screw is provided for measurements. The backlash is considered by measuring slit width by travelling microscope during closing and opening of the slit.

5.2 WAVELENGTH CALIBRATION

Mercury and sodium lamps are used for the preliminary setting of wavelengths. However, the resolution of the system is determined by measuring the sun and the sky spectra reflected by freshly prepared MgO screen and plane mirror. The sky and the sun spectra are the best sources for testing the resolution as well as wavelength calibration, as these spectra contain absorption lines with different bandwidths i.e. from milliangstroms to angstroms.

6. MONITORING OF ATMOSPHERIC GASES :

The different atmospheric gases which can be monitored by this system depend upon the following parameters.

i. The absorption band of the gas molecule must lie in the spectral range of the spectrometer i.e. 0.3 μ to 0.8 μ (using photomultiplier tube as detector).

ii. – The product of the number of molecules to be monitored measured and the absorption cross section of the species is measuring factor for the absorption.

This product should lie in the detection range ($\lesssim$ 0.02% absorption), with these criteria the number of gases which can be monitored in different modes of measurement using the system is given in Table 3. This table gives the different tropospheric and stratospheric gases those can be monitored, the different type of sources and the resolution used by some other workers. As the throughput of our system is higher compared to that of other workers, the higher resolution can be achieved and the gases like NO_2, CH_4, O_3, SO_2, CH_2O, H_2O, OClO, BrO ... etc can be monitored with the present design of the system (Noxon et al., 1978, 1979; Platt et al., 1979, 1980, 1981, 1982, 1984; Solomon et al., 1987).

Table 3 : List of atmospheric constituents to be monitored using visible spectrometer

Species	Wavelength range	Reference	Source	Accuracies achieved	Resolution	
					By other workers	By our system
NO_2 (S, T)	0.435-0.450 u	Noxon 1978	Sun	0.015 ppb	7A	4A
			Sky	1×10^{15}	7A	
O_3 (S, T)	0.430-0.450 u	Solomon et al. 1987	Sky	1×10^{18}	4A	4A
NO_3 (S, T)	0.623-0.662 u	Noxon et al. 1978	Moon	0.8×10^{14}	7A	4A
CH_2O (T)	0.326, 0.339 u	Platt and Perner 1980	Xenon/	0.1 ppb	5A	0.2 A
HNO_2 (T)	0.354, 0.368 u	Platt et al., 1984	Tungsten	0.02 ppb	5A	0.2 A
NO_2 (T)	0.375, 0.365 u	"	Iodine	0.08 ppb	5A	0.2 A
O_3 (T)	0.328 u	Platt et al., 1979	Lamp	1.2 ppb	5A	0.2 A
SO_2 (T)	0.300 u	"		0.01 ppb	5A	0.2 A
NO_3 (T)	0.623-0.662 u	"		0.0005 ppb	5A	0.2 A

S - Stratospheric T - Tropospheric

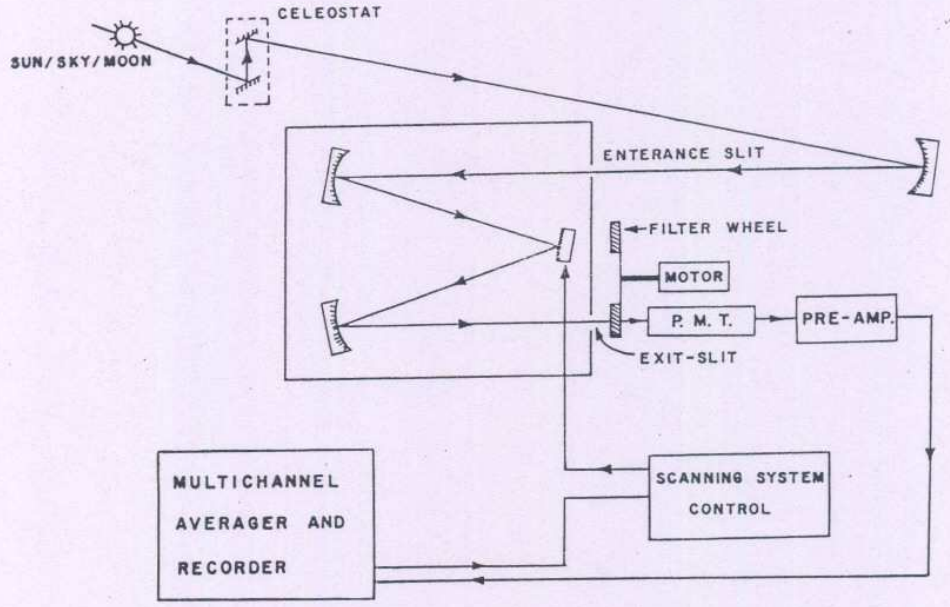

HIGH RESOLUTION VISIBLE SPECTROMETER FOR ATMOSPHERIC STUDIES

FIGURE 15

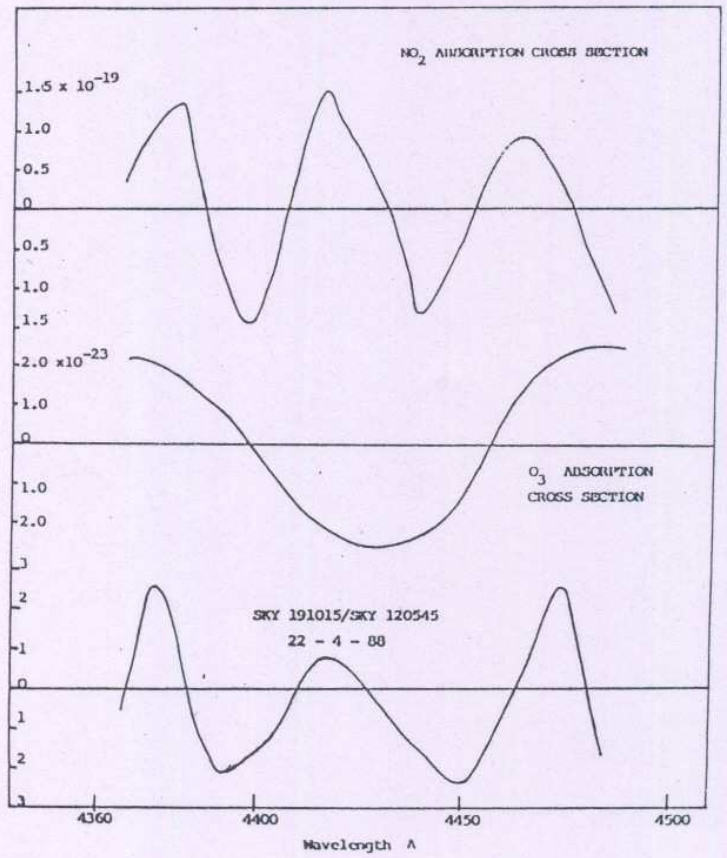

FIGURE 16

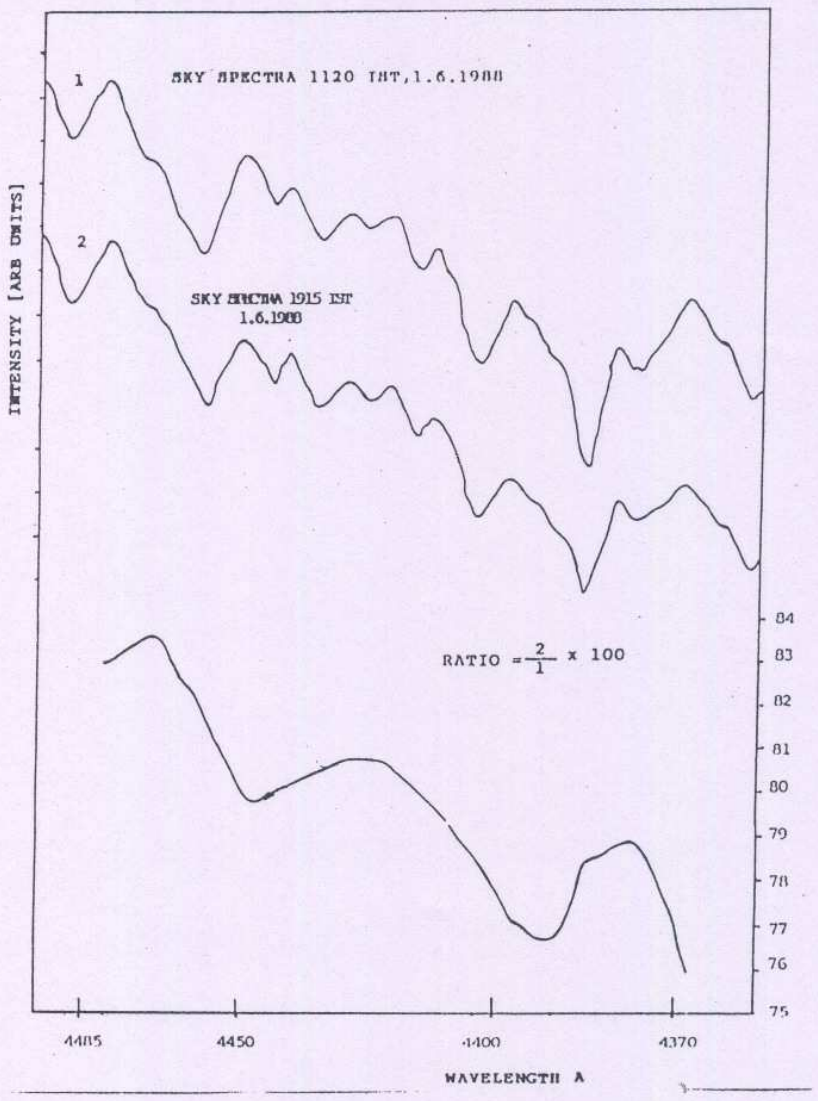
1
SKY SPECTRA 1120 IST, 1.6.1988
2
SKY SPECTRA 1915 IST
1.6.1988
INTENSITY [ARB UNITS]
RATIO = 2/1 x 100
84
83
82
81
80
79
78
77
76
75
4485
4450
4400
4370
WAVELENGTH A

FIGURE 17

7. OBSERVATIONS OF TOTAL COLUMN DENSITY OF NO_2 & O_3

To begin with, the preliminary observations were carried out for total column density of NO_2 and O_3 at Pune during clear sky twilight hours. The observational arrangement is shown in Fig 15. The zenith sky spectra for spectral region 4360 A to 4450 A were obtained during noon time and evening time. The percentage absorption depth due to NO_2 and O_3 was obtained by taking the ratio of the two zenith sky spectra. The Fraunhofer line structure present in the observed spectra is automatically eliminated by the ratio technique. Fig. 16 shows the laboratory absorption cross sections for NO_2 and O_3 separately. Fig. 17 shows the observed spectra and the resultant spectra obtained by taking ratio. By using the matrix inversion techniques the contribution of NO_2 and O_3 to the percentage depth can be separated and the difference in number of molecules for NO_2 and O_3 can be obtained. The detailed analysis procedure for these calculations is given elsewhere (Mehra et al., 1989).

CONCLUSIONS

i. It is possible to design and develop the high resolution UV - visible spectrometer using most of the indigenious components.

ii. At high resolution the use of curved slits in place of straight slits allows the increase in the throughput by a factor of 60.

iii. High and low pass square wave pass type of transmission filters are very useful as order sorting filters.

iv. The maximum resolution can be achieved by this system is from 6 mA to 50 mA from 0.3 μ to 0.8 μ spectral region.

v. Using multichannel averager/control and data processing system with spectrometer the wide range of the source intensities from night sky radiation to solar radiations can be studied.

vi. The stratospheric species (like NO_2, NO_3, O_3, OClO, BrO) and the tropospheric species (like NO_2, HNO_2, NO_3, O_3, SO_2, CH_2O, HO_2 etc) can be monitored with the above system using sources like the Sun, the Moon, Sky, or artificial sources like Xenon lamp or Tungsten Iodide lamp.

ACKNOWLEDGEMENTS

The authors wish to thank Shri D.R. Sikka and Dr. A.S.R. Murty for their continuous encouragement during this work. Their special thanks to Shri K.G. Vernekar and the referees for the valuable suggestion and also to Dr. S.S. Parasnis for the discussions during the preparation of the report.

REFERENCES

Badger, Z. and Giguere. 'A vaccum spectrograph for infrared'. Rev. Sci, Inst. 19, 861, 1948.

Bosch and Lomb. 'diffraction gratings catalogue', 1982.

Carli, B.F. Mencaraglia, A. Bonetti. 'Fourier Spectroscopy of the stratospheric emission'. Int. J. Infra Red m.m. waves. 3, 385-394, 1982.

Coffey, M.T., W.G. Mankin, and Goldman. 'Simultaneous spectroscopic determination of the latitudinal, seasonal and diurnal variability of stratospheric N_2O, NO, NO_2 and HNO_3'. J. Geophys. Res., 86, 7331-7341, 1981.

Corion Carporation, 'Optical filter and coating', Catalogue, 1983.

Czerny and Turner. 'Astigmatism in mirror spectrometers', Zeits, F. Physik, 61, 792, 1930.

Ebert. Wied, Ann. 38, 489, 1889.

Fastie W.G. 'A small plane grating monochromator', J. Opt. Soc. Am. 43, 1174, 1953.

Fastie W.G. 'Experimental performance of curved slits', J. Opt. Soc. Am. 43, 1174, 1953.

Fastie W.G. 'Ultraviolet measurements in planetary atmosphere', Appl. Opt. 6, 397, 1967.

Girad, A., na. N. Louisnard. 'Stratospheric water vapour, NO_2 Nitrogen dioxide, Nitric acid and ozone measurement deduced from spectroscopic observations'. J. Geophys. Re. 89, 5109-5114, 1984.

Hammamatsu, Photomultiplier tube, Catalogue, 1988.

Husson N., A. Barbe., H.M. Pickett., L.R. Brown; A.E. Roche., B. Carli., L.S. Rotham., A. Goldman., M.A.H. Smith. 911-949 Atmospheric ozone, W.M.O. Report No. 16, 1985.

Jadhav D.B. 'Selection of optical spectrometers'. J. Opt. 14, 76-84, 1985.

Jadhav D.B., A.D. Tillu. 'Design and fabrication of high light gathering power monochromator', J. Opt. 15, 54-61, 1986.

James, J.F., and R.S. Sternberg. 'The design of optical spectrometers', (Book) (Chapman and Hall, London), 1969.

Londhe A.L., H.K. Trimbake., S.D. Bhonde and D.B. Jadhav. 'Preliminary observations of total column density of Nitrogen dioxide over Pune', Symp., NGRI, Hyd. 8-10 Feb, 1989.

McKenzie R.L., and P.V. Jhonston. 'Seasonal variation in stratospheric NO_2 at 45 degrees S.', Geophys. Res. Lett. 9, 1255-1258, 1982.

Mehra Poonam. 'Measurement of total columnar density of NO_2 and O_3 using twilight visible spectroscopy'. National Space Science Symp. Feb. 1990.

Murcray, D.G., A. Goldman., J. Kosters., R. Zander., W. Evans., N. Louisnard., C. Alamichel., M. Bangham., S. Pollitt., A. Volboni., W. Traub & K. Chance. 'Inter comparsion of stratospheric water vapour profiles obtained during the balloon intercomparison campaign.' Atmospheric ozone', D. Riedel publication, Dardrecht, 1985a.

Noxon, J.F., R.B. Norton. and W.R. Henderson, 'Observation of atmospheric NO_3', Geophys. Res. Lett. 5, 675-678, 1978.

Noxon, J.F. 'Tropospheric NO_2', J. Geophys. Res. 83, 3051-3057, 1978.

Noxon, J.F., E.C. Whipple Jr. and R.S. Hyde. 'Stratospheric NO_2 No. 1 observational method and behaviour at mid-latitude', J. Geophys. Res. 84, 5047-5056, 1979.

Platt, U., Perner, D., and Patz, H.W. 'Simultaneous measurement of atmospheric CH_2O, O_3 and NO_2 by differential optical absorption', J. Geophys. Res., 84, 6329-6335, 1979.

Platt, U. and D. Perner. 'Direct measurements of atmospheric CH_2O, HNO_2, O_3, NO_2 by differential optical absorption in the near UV'. J. Geophys. Res., 85, 7453-7458, 1980.

Platt, U.G.,D. Perner., A.M. Winer., G.W. Harris. and J.N. Pitts. 'Detection of NO_3 in the polluted troposphere by differential optical absorption', Geophys. Res., Lett., 7, 1, 89-92, 1980.

Platt U.F., D. Perner., J. Schroder., V. Kessler. and A. Toennissen. 'The diurnal variation of NO_3'. Jr. Geophys. Res. 86, C12, 11965-11970, 1981.

Platt, U.F.,A.M. Winer., H.W. Biermann., R. Atkinson. and J.N. Pitts. Jr. 'Measurement of Nitrate Radical Concentrations in Continental Air'. Environment Science and Technology, 18, 365-369, 1984.

Rowland F.S., D.R. Blake. and E.W. Mayer. 'World wide increase in concentration of atmospheric methane since 1978', in Symposium proceedings of WMO Technical Conference on observation and measurement of Atmospheric contaminants.

Sassa, N., Science of Light 10, 53, 1961.

Solomon. S., A.L. Schmeltekopf. and R.W. Sanders. 'On the Interpretation of zenith sky absorption measurements'. J. Geophys. Res. 92, D7, 8311-8319, 1987.

Syed. M.Q. and A.W. Harrison, 'Ground based observations of stratospheric Nitrogen dioxide', Canad. Jr. Phys. 58, 788-802, 1980.

Thorne A.P., 'Spectrophysics (Book)', Chapman and Hall, London. 1974.

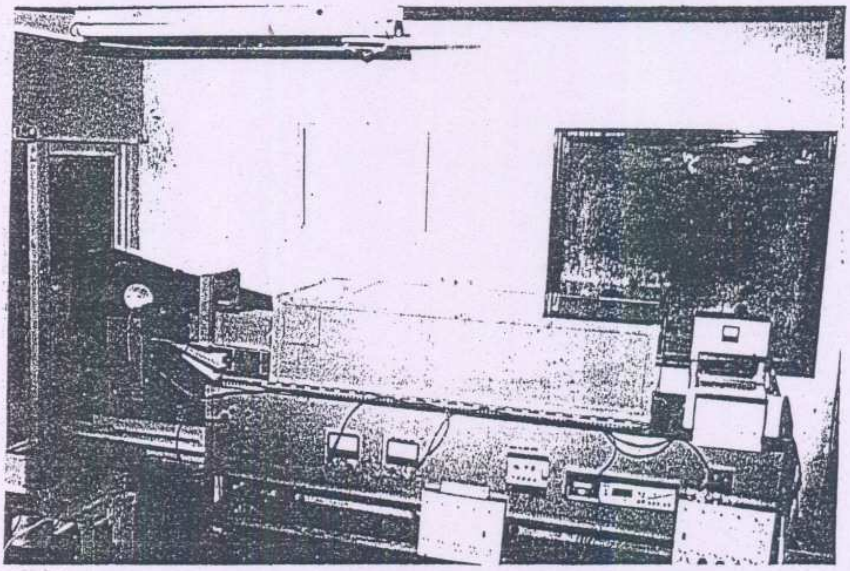

HIGH RESOLUTION UV - VISIBLE SPECTROMETER
FOR ATMOSPHERIC STUDIES